HTD-Vol. 343

ASME Proceedings of the 32nd

NATIONAL HEAT TRANSFER CONFERENCE

VOLUME 5

• THERMAL MANAGEMENT OF HAND-HELD, WEARABLE AND PORTABLE ELECTRONICS

presented at

THE 32nd NATIONAL HEAT TRANSFER CONFERENCE
BALTIMORE, MARYLAND
AUGUST 8–12, 1997

sponsored by

THE AMERICAN SOCIETY OF MECHANICAL ENGINEERS, ASME
THE AMERICAN INSTITUTE OF CHEMICAL ENGINEERS, AIChE
THE AMERICAN INSTITUTE OF AERONAUTICS AND ASTRONAUTICS, AIAA
THE AMERICAN NUCLEAR SOCIETY, ANS

edited by

CRISTINA H. AMON
CARNEGIE MELLON UNIVERSITY

CHRISTIAN BELADY
HEWLETT-PACKARD COMPANY

MICHAEL BOYLE
UNIVERSITY OF MAINE

CSILLA HERMAN
JOHNS HOPKINS UNIVERSITY

SUNG JIN KIM
IBM STORAGE SYSTEMS

SERI LEE
AAVID THERMAL TECHNOLOGIES

ALFONSO ORTEGA
UNIVERSITY OF ARIZONA

SAJEEV SATHE
IBM CORPORATION

BAHGAT SAMMAKIA
IBM CORPORATION

THE AMERICAN SOCIETY OF MECHANICAL ENGINEERS
United Engineering Center • 345 East 47th Street • New York, N.Y. 10017

HTD-Vol. 343, National Heat Transfer Conference
Volume 5
ASME 1997

EXPERIMENTAL STUDY OF CONJUGATE HEAT TRANSFER IN A HORIZONTAL CHANNEL WITH DISCRETE HEATED CUBIC BLOCKS

W. Tang and A. J. Ghajar
School of Mechanical and Aerospace Engineering
Oklahoma State University
Stillwater, Oklahoma 74078

ABSTRACT

Heat transfer measurements were taken in a horizontal rectangular wind tunnel in turbulent flow with an in-line array of highly polished aluminum cubes of 2.54 cm. Experiments were conducted at four velocities (5, 7, 9 and 11 m/s) for three channel heights (7.62, 5.08 and 3.81 cm). One single aluminum cube was heated (10 or 20W) at a time on six different conductive test boards to quantitatively investigate the conduction effects of the surface area and thickness of the copper foil in a single-sided printed circuit board. To simulate conjugate heat transfer phenomena, pre-cut copper clad circuit board blanks of two different thicknesses were etched with the same designed pattern but different copper foil band widths which reflect different exposed copper foil surface areas. An adiabatic board consisting of a bare printed circuit board without any copper foil on it was also used as a base-line case. Empirical correlations based on the experimental heat transfer results of this study were developed. A modified Reynolds number was used in the correlations. It absorbs the channel height parameter by calculating a modified velocity generated by variation in channel cross sectional areas associated with different channel heights. Two new parameters were also introduced in the correlations to reflect the conduction effect of the copper foil in the PCBs. The first one is the ratio of exposed copper foil surface area ratio (A^*). The second one is the copper foil thickness ratio (T^*). These two new parameters (A^* and T^*) together with the modified Reynolds number and the non-dimensional channel height (H/t) were identified as the most important parameters under the configuration of the study.

NOMENCLATURE

A^*	exposed copper foil surface area ratio, dimensionless
$A_{blocked}$	the cross sectional area of the channel blocked by the aluminum modules, cm^2
A_{cross}	cross sectional area of the rectangular channel, cm^2
A_m	exposed module surface area, cm^2
D_h	hydraulic diameter of the channel, cm
H	rectangular channel height, cm
h	heat transfer coefficient, W/m^2-K
k	thermal conductivity of the cooling air at T_∞, W/m-K
Nu	Nusselt number (= ht/k), dimensionless
$Nu_{1\,oz}$	Nusselt number of 1 oz conductive test boards
$Nu_{2\,oz}$	Nusselt number of 2 oz conductive test boards
Nu_{ad}	Nusselt number of the adiabatic test board
Q_k	vertical conduction heat loss, W
Q_m	equivalent (lumped) convection heat transfer rate of the heat dissipating module, W
Q_r	radiation heat loss, W
Q_t	input power to the active (heat dissipating) module, W
Re	modified Reynolds number (= V^* t/ν), dimensionless
R_w	thermal resistance of the test board and channel floor assembly, °C/W
T*	copper foil thickness ratio, dimensionless
T_∞	approaching cooling air temperature of the test fluid or the surroundings air temperature, °C
T_m	module temperature, °C
t	module height, (2.54 cm), cm
V	measured channel centerline velocity, m/s
V^*	modified channel centerline velocity (see Eq. (6)), m/s
x	stream-wise distance from the center of a module to the beginning of the in-line array, m
ε	emissivity of polished aluminum, (0.06), dimensionless
ν	kinematic viscosity of the cooling air at T_∞, m^2/s

Subscripts

exp	refers to the experimental value
pred	refers to the predicted value

INTRODUCTION

Electronic devices have become a vital part of modern civilization. The circuit density of electronic components has steadily increased. Accordingly, the power dissipation of each succeeding generation of electronic equipment has been creating

greater and greater demand on effective cooling technology. The effective cooling of electronic equipment relies upon the thorough understanding of all the physical factors involved under different circumstances. This research focuses on the combined modes of conduction and convection heat transfer from a single-sided air-cooled printed circuit board (PCB) with heat-dissipating electronic components. It is common that these electronic components are arranged in in-line arrays on a PCB. With some idealizations and simplifications, a horizontal rectangular channel with a regular in-line array of cubic modules, which are frequently used to represent typical PCB topologies, are studied in this paper.

Heat transfer in electronic cooling is a topic that has generated a lot of interest among researchers in recent years. Consequently, this has lead to many research directions and a great variety of studies have been published. Only the works related to the present experimental study in the published literature are cited here. All describe experimental studies of conjugate heat transfer from PCBs populated by either a single surface mounted block or an in-line array of blocks that represent simulated electronic components positioned in a rectangular channel.

Biber and Sammakia (1986) made extensive heat transfer measurements in an array of 20 real PCBs, each densely populated with heat-dissipating modules that could be arbitrarily heated. Three sizes of modules were investigated and each PCB was populated with an array of uniform sized modules. There were two different PCB versions, one with two 0.003 in. copper power planes (copper foil) and one without. It was observed that in real PCBs, conduction effects were always important because of the presence of copper power distribution planes within the board.

Graham and Witzman (1988) carried out experiments to supplement their analytical study of thermal design of electronic packages. Their experiments covered many component package (semiconductor chip in an electronic package) styles. FR4 type PCBs and smaller FR4 test coupons were used. These authors discovered that in many designs, 40 to 60 percent of the total heat load would be dissipated through the board into the air stream.

Azar and Moffat (1991) conducted an experimental investigation to measure the heat transfer coefficients on twelve representative components in a simulated electronic circuit pack. They found that the thermal behavior of the simulated electronic circuit pack was strongly affected by conduction, with conduction to the PCB accounting for between 20 to 60 percent of the total power dissipation.

Arabzadeh, et al. (1993) examined the effect of Reynolds number, component placement, and board conductivity on the conduction heat transfer to the board, component temperature, and convection heat transfer coefficient. Experiments were conducted in a horizontal rectangular wind tunnel using an array of twelve components. Three test boards were used to investigate the board conductivity effect. The experimental results indicated that the conduction heat transfer through the board and consequently the thermal behavior of the system were strongly affected by the Reynolds number of the flow, placement of the component, and the board conductivity. They concluded that board conductivity can have significant direct effect on the operating temperature of the heated component.

Lohan and Davies (1996) conducted an experimental study by measuring the forced-air junction-to-ambient thermal resistance of a single 160-lead plastic quad flat pack electronic component mounted on a standard SEMI test PCB. The same approach was also applied to a regular in-line array of the same type of components mounted on a larger Double Euro Card test PCB. Copper tracking covered 19% of the total surface area of both PCBs. Several experiments were conducted with and without non-component side insulation. The most influential factors that contributed to an increase in component resistance were the loss of convective heat dissipation from the PCB's non-component side and the existence of powered adjacent components.

Nakayama and Park (1996) investigated both experimentally and analytically the conjugate heat transfer from a single surface-mounted block to forced convective air flow in a parallel-plate channel. A simulated module consisted of a copper piece supported by various materials with the same dimensions. The channel floor was tested with different materials as well. They concluded that the thermal resistance of the block support is an important parameter that controls the conjugate heat transfer from the floor. It was also found that a good thermal bonding between the block and the floor, with the support's resistance of the order of 0.01 K/W, and a high thermal conductance of the floor, maximizes the conduction heat transfer from the module to the floor to more than 50%.

All the investigators mentioned above have studied the conjugate heat transfer problem of electronic cooling by conducting experiments on either simulated or real PCBs. In general, the conclusions they reached were (1) conduction can be a significant part of PCB conjugate heat transfer, (2) the higher the thermal conductivity of the substrate, the greater the influence of conduction and some researchers also found that (3) the lower Reynolds number, the greater the influence of conduction. The shortcomings of their studies are summarized as follows:

(1) All the simulated PCBs tested consisted of different materials and fabricated using different contrived techniques. As no two simulated boards were the same, the scope for comparing results was hampered.

(2) With the exception of Lohan and Davies (1996) who qualitatively showed that greater exposed copper foil area promoted conduction heat spread, the majority of experimental studies that used real PCBs failed to examine the important characteristics of PCB conduction heat transfer. For example, the effects of exposed copper foil surface area, the thickness of the copper foil, etc.

Systematic and quantitative studies on the important heat transfer characteristics of real PCBs are needed to understand this complex subject. This study applied the copper etching method to produce different effective conductivity test boards with different exposed copper foil band widths and different copper foil thicknesses. This approach enabled one to quantitatively study the effects of different conductivity substrates on the conjugate heat transfer process. By introducing copper clad circuit board blanks and the making of test boards with etching method to electronic

cooling research; it is our hope that some unintended confusion of the material and construction of the test boards can be avoided in the future.

EXPERIMENTAL SETUP AND PROCEDURES

A schematic diagram of the experimental apparatus for the heat transfer measurements is shown in Fig. 1. This experimental setup was built and instrumented by Arabzadeh (1993). The uncertainty analysis of the overall experimental procedures using the method of Kline and McClintock (1953) showed that there was a maximum of 3.8% uncertainty for heat transfer coefficient calculations. The same analysis was applied to the channel centerline velocity measurement and showed a maximum of 7.7% uncertainty for all the velocity measurements.

A total of six conductive boards were made for the study with three different copper band widths which simulate the different exposed copper foil surface areas of PCBs in real applications. Half of the boards had a 1 oz (0.0034 cm) thickness with three band widths and the other half had a 2 oz (0.0068 cm) thickness with the same three band widths as the 1 oz boards. The copper foil distribution pattern was exactly the same for all the conductive boards. One bare PCB without any copper foil was also tested as the base-line case for comparison purposes. For the six conductive test boards, PCB blanks (1 and 2 oz, FR-4) were etched with the same pattern but different band widths to generate different copper foil covered surface areas. This method was applied in the present experimental study to investigate the conduction effects of the copper foil in the PCBs which has not been focused on in previous research.

Pre-cut copper clad circuit board blanks (25.4 × 38.1 cm) were exposed with an ultra violet fluorescent light source, developed in a heated solution, and then etched in the Ferric Chloride etchant with constant agitation to produce the conductive test boards with the designed copper foil distribution pattern on them. The pattern was separated copper foils of 2.54 cm squares connected by a uniform width of 2.54, 1.27 or 0.318 cm in the same length (2.54 cm) of copper foil bands both in stream-wise and span-wise directions. Schematics of the finished test boards are shown in Fig. 2 in which the three copper foil band widths with the same designed pattern can be clearly seen for the conductive test boards. Tested modules were mounted on the floor of a 152.4 cm long rectangular channel with a fixed width of 25.4 cm and the height of the rectangular channel was adjustable from 1.27 to 7.62 cm. The rectangular channel was constructed of 1.27 cm commercial grade plexiglas. Ambient air entered the rectangular channel through a 101 cm long wooden contraction smoothing the flow of the incoming air. Inlet to outlet ratio of the contraction varied from 14.5 to 82, depending on the channel height. For any desired channel height, an appropriate flow straightener corresponding to the channel height was installed at the entrance of the rectangular channel to produce a uniform velocity profile. Flow straighteners consisted of soda straws (0.55 cm inside diameter, 12 cm in length) tightly packed between galvanized steel mesh screens (0.044 cm wire diameter, 0.32 cm mesh width). Leading row of the test module array was positioned 76.2 cm from the entrance of the rectangular channel and the array extended for 38.1 cm downstream. Top and side views of the test section encompasses an array of modules arranged in a regular in-line pattern as illustrated in Fig. 3. Span and stream-wise inter module spacings were equal (2.54 cm). Cubic module planform dimension L is also 2.54 cm as indicated in the top view. Module height t (2.54 cm) and channel height H (7.62, 5.08 and 3.81 cm) of the flow passage are indicated in the side view. Each test board used in the test section was mounted with eight rows and four columns of full-size (2.54 cm cube) modules flanked on both sides (in the flow direction) by half-size (2.54×1.27×2.54 cm rectangular aluminum block) modules. Each half-size module was mounted on the side wall adjacent to the channel floor. Idea underlying the employment of the half-size modules is to simulate an infinite wide array more closely (Sparrow, et al., 1982). Referring to Fig. 3 only the temperatures of the three columns (24 modules) in the flow direction with darker shade were monitored and recorded during the experiments. Modules which were heated one at a time were the first five modules (rows 1 to 5) in the center column of the three columns with darker shade.

Ambient air was drawn past the test modules by a 2 HP variable speed blower mounted downstream of a wooden plenum. The rectangular channel emptied to the acoustically absorbent wooden plenum that served to isolate the air flow past the test section from the blower noise. Air velocity (channel centerline velocity) was measured by a pitot static tube positioned 6.4 cm upstream of the leading row of test modules and controlled (four velocities for present study, 5, 7, 9 and 11 m/s) at the blower's end of the circular duct between the plenum and the blower by a computer controlled wooden damper/stepper motor arrangement. Pitot static tube used to measure the channel centerline velocity at the test section was connected to a differential pressure transducer. Electronic components were modeled by highly polished aluminum cubes (2.54 cm) with a thermal conductivity of 216 W/m-K. Every tested module was equipped with a thermocouple and electric resistors as the internal power source. The resistor was placed at the center of each test module in a cavity. Then the cavity was filled with a thermally conductive epoxy. In-line array of aluminum modules were then mounted on a test board with nylon bolt and nuts. A detailed plan view of a cubic aluminum module and a typical assembly of the test board on the channel floor used in the study is shown in Fig. 4. Power delivered to each module was manually controlled by a DC power supply. Power was constantly monitored and measured by two multimeters so that the desired power levels of 10 or 20W could be constantly supplied with a maximum uncertainty of 1.5%.

Each experimental run began with installing the desired test board with the in-line array of test modules in the test section, then connecting the power supply leads of the selected module to the power supply unit and the thermocouple wires of all the monitored modules to the digital data logger. Blower was turned on after the entire rectangular channel was sealed, then the power supply unit was turned on and the channel centerline velocity was controlled through a PC to reach the desired velocity. As mentioned previously, input power to the selected module was manually controlled to the desired value during the experiment. Temperature of the heated module was monitored every five minutes until the steady state condition defined by a variation in temperature of no more than ±0.1°C was reached. It generally took 20 to 30 minutes to reach steady state depending on the channel centerline velocity. Steady state temperatures of the heat dissipating module and the rest of the twenty-three passive

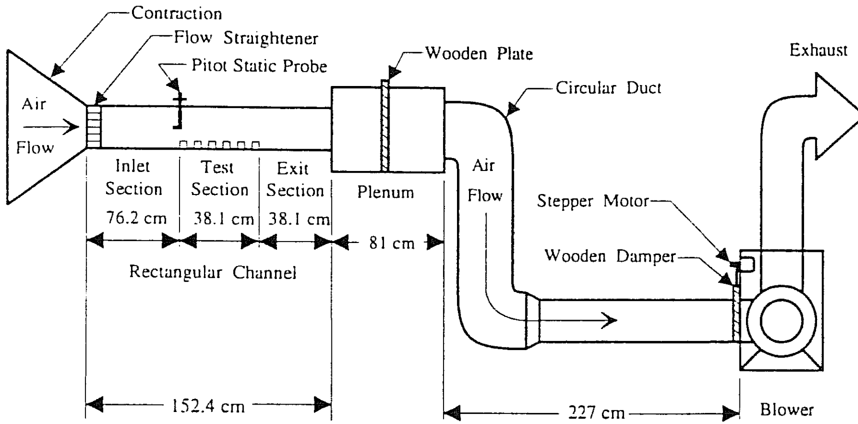

Fig. 1 Schematic of the experimental apparatus.

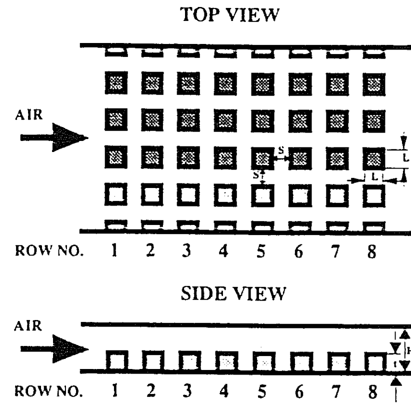

Fig. 3 Schematics of the top and side views of the the test section with an in-line array of cubic modules (on the adiabatic test board) used in the study (S = L = 2.54 cm, t = 2.54 cm and H = 7.62, 5.08 or 3.81 cm).

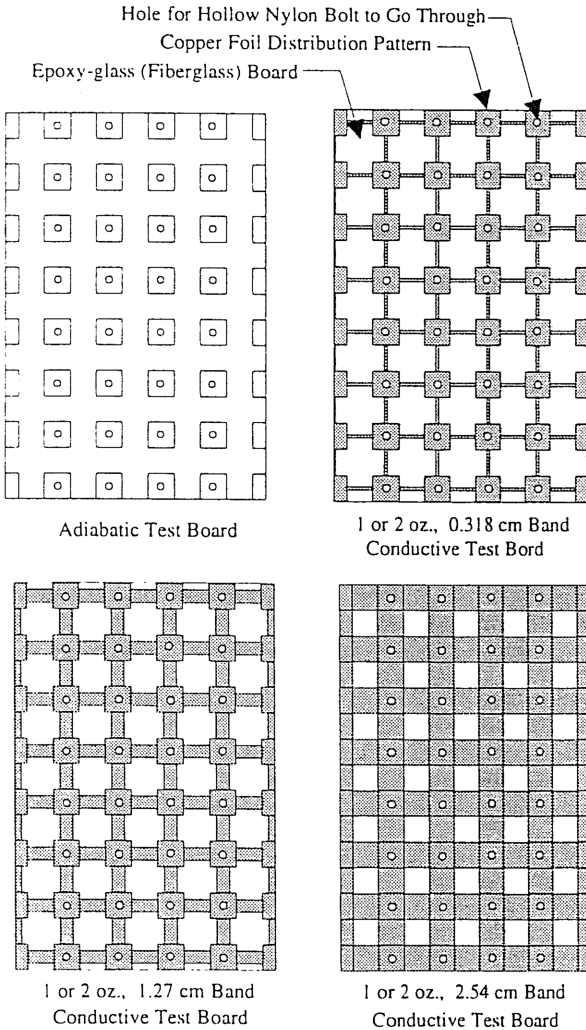

Fig. 2 Top view of four different test boards with the same dimensions of 25.4 by 38.1 cm.

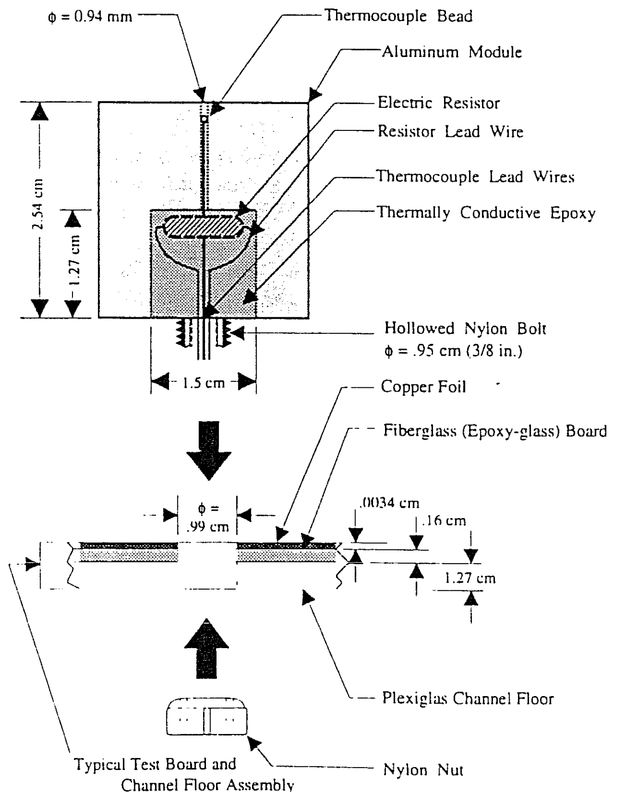

Fig. 4 Detailed plan-view of a full-size cubic aluminum module and a typical test section channel floor assembly.

modules monitored were recorded and stored in the PC. Estimated vertical conduction loss from the heat dissipating module through the channel floor, estimated radiation heat loss, and convection heat transfer coefficient of the heat dissipating module were then calculated from the recorded data.

As the test air velocities were quite high, the vertical conduction heat losses through the rectangular channel floor (Q_k) were relatively small compared with the convection heat transfer. Radiation heat losses to the surroundings (Q_r) were estimated using a simple basic model (Stefan-Boltzmann law with $\varepsilon = 0.06$, Kraus and Bar-Cohen, 1983). For the estimated vertical conduction heat loss through the channel floor, separate experiments with different board material with different thermal conductivities, were performed on the same experimental setup (see Arabzadeh et al., 1993). These experiments demonstrated that a board composed of plexiglas and fiberglass can be considered as a non-conductive board, and one-dimensional conduction calculation would be sufficient (in vertical direction, a layer of copper foil on top of the fiberglass board would not change the conclusion). Thus, the estimated conduction heat loss through the channel floor assembly was calculated by

$$Q_k = (T_m - T_\infty) / R_w \qquad (1)$$

where T_m is the heat dissipating module temperature, T_∞ is the approaching air temperature measured at the entrance of the rectangular channel with a T-type thermocouple connected to the digital data logger. Neglecting contact resistance, $R_w = 111$ °C/W is the thermal resistance of the test board and channel floor assembly right under the heat dissipating module based on the bottom plan area of the module. A steady state energy balance on the control volume surrounding a module yields the convective heat release as:

$$Q_m = Q_t - Q_k - Q_r \qquad (2)$$

The lateral conduction heat flow from the heat dissipating module eventually finds its way to the cooling air flow through the four connecting copper foil bands of the heat dissipating module and the neighboring modules. After subtracting the estimated vertical conduction heat loss (Q_k) through the channel floor and radiation heat losses (Q_r) from the input power (Q_t) supplied to the heated module, Q_m is used to calculate the convection heat transfer coefficient. That is, in this study, the lateral conduction heat flow from a heat dissipating module is lumped together with the convection heat transfer from the exposed surfaces of the module itself to calculate an equivalent heat transfer coefficient (h) and the corresponding Nusselt number (Nu). The equivalent convection heat transfer coefficient of the heat dissipating module can be calculated by

$$h = Q_m / A_m (T_m - T_\infty) \qquad (3)$$

where A_m is the exposed surface area of the heat dissipating module. The corresponding Nusselt number is found by

$$Nu = ht/k \qquad (4)$$

where the height of the module, t (2.54 cm), is the defined characteristic length of the experiments and k is the thermal conductivity of the cooling air flow. The thermal conductivity of the cooling air is determined based on the average approaching air temperature (T_∞) for a specific experimental run. The maximum ratio of Q_k/Q_m was found to be 4.6%, and the maximum ratio of Q_r/Q_m was 1.0% in the study. Both happened on the adiabatic test board and at the lowest channel centerline velocity of 5 m/s and highest channel height of 7.62 cm.

RESULTS AND DISCUSSION

This section presents the heat transfer results for forced convection in a channel containing an in-line array of aluminum cubes on six conductive boards and one baseline adiabatic board. The modified Reynolds number of the study is defined as

$$Re = V^* t / \upsilon \qquad (5)$$

where v is the kinematic viscosity of air evaluated at T_∞, t is the characteristic length of the study (the module height, 2.54 cm) and V* is the modified centerline velocity which is defined as

$$V^* = V\, A_{cross} / (A_{cross} - A_{blocked}) \qquad (6)$$

where V is the channel centerline velocity, A_{cross} is the cross sectional area of the rectangular channel and $A_{blocked}$ is the cross sectional area of the channel blocked by the aluminum modules (5×2.54^2 cm^2). The range of the modified Reynolds numbers was between 9100 to 26300 in the study. Accordingly, the flow regime for the entire experiments conducted in this study was turbulent based on Reynolds number.

The characteristic length was chosen as the height of the module t in the study. The other possible choices, channel height H and the spacing that the free stream passes H-t, were not chosen because using either one of them would result in undesirable trend of the Reynolds number. For example, as the channel height increased, the Reynolds number would increase if the channel height (H) or the free stream pass spacing (H-t) was used as the characteristic length. However, the experimental data indicated clearly that the Nusselt number actually decreased if the channel height increased. In order to avoid these two contradictory trends in the study, the characteristic length was chosen to be the module height (t). It remained the same for the three different channel heights. To accommodate the effects of channel height variations, the modified centerline velocity (V^*) was used in the definition of Reynolds number for this study.

To systematically and quantitatively study the heat transfer characteristics of the copper foil present in a PCB, experiments were conducted to investigate several parameters of this conjugate problem. These parameters include:

- Exposed surface area of copper foil. There were three band widths, 2.54, 1.27 and 0.318 cm with $A^* = 0.682$, 0.341 and 0.085 respectively.
- Thickness of copper foil. There were two thicknesses, 1 oz (0.0034 cm) and 2 oz (0.0068 cm).
- Modified Reynolds number (from 9100 to 26300).
- Channel height (7.62, 5.08 and 3.81 cm).
- Heat dissipating module position (row number 1 to 5).

Figures 5 to 14 and Tables 1 to 3 illustrate the results of the study related to these parameters. A schematic of the top view of the in-line array of modules on a test board is included to help demonstrate the results. In the schematic, the modules with darker shades are the modules that were heated one at a time during the experiments. The copper bands of a typical conductive test board connecting all the modules were also shown in the schematic. The

adiabatic test board was not illustrated graphically because of limited space. The only difference between two types (adiabatic and conductive) of test boards is that the conductive boards have conductive paths (copper bands) connecting every module in the array, while the adiabatic board has none. Effects of these parameters are discussed in details in the following sections.

Effect of Channel Centerline Velocity on Nusselt Number

Figure 5 shows the Nusselt numbers versus row number parametric in channel centerline velocity (V) on three 1 oz and the adiabatic test boards for a fixed channel height of 7.62 cm. Data of three 2 oz conductive and the adiabatic test boards are displayed in Fig. 6. As shown in Figs. 5 and 6, the Nusselt numbers increased with increasing centerline velocity V for a fixed channel height H. This trend can be consistently observed for all test boards at all three channel heights. The same trend has been documented by both Moffat et al. (1985) and Wirtz and Dykshoorn (1984) for adiabatic cases. Therefore, it can be concluded that in turbulent flow regime, forced convection heat transfer is still the dominant mechanism of this conjugate heat transfer process on all three conductive test boards of the study.

Effect of Channel Height on Nusselt Number

Figure 7 shows the Nusselt numbers versus row number parametric in channel height (H) on three 1 oz conductive and the adiabatic test boards for a fixed channel centerline velocity of 5 m/s. Figure 8 shows the data of three 2 oz conductive and the adiabatic test boards. The opposite trend to what was shown in Figs. 5 and 6 could be observed for decreasing channel height and a fixed centerline velocity as shown in Figs. 7 and 8. Again, similar results were found for different channel centerline velocities. With decreasing channel height H, the Nusselt numbers increased for a fixed centerline velocity V. This trend was also reported by Moffat et al. (1985) for cubic modules and adiabatic cases. Results shown in Figs. 5 to 8 lead to the conclusion that both channel centerline velocity and the channel height are two essential parameters in the study. The effects of both parameters were consistent without any exception for all the experiments. For any test board, conductive or adiabatic, the increase of centerline velocity would always result in higher Nusselt number of the heat dissipating module at a fixed channel height. For any test board, the decrease of channel height would always result in higher Nusselt number of the heat dissipating module at a fixed centerline velocity as well. It should also be pointed out that both the increase of the centerline velocity and the decrease of channel height would increase the modified Reynolds numbers of the experiments.

To demonstrate this trend numerically, some examples of two selected modules are given in Table 1 for two selected velocities (5 and 11 m/s) and three test boards (1 oz and 2 oz, 2.54 cm band, and adiabatic). Table 1 confirmed that for both the conductive and adiabatic test boards, the influence of channel height was consistent. With decreasing channel height H, the Nusselt numbers increased for a fixed centerline velocity V.

Effect of Exposed Copper Foil Surface Area Ratio on Nusselt Number

When a module was heated on any conductive test board of the study, part of the heat would be dissipated through the bottom surface (2.54^2 cm^2) of the module to the copper foil by conduction and then found its way to the cooling air flow. Most of that heat was conducted vertically through the bottom surface of the heated module to the copper foil then, would be distributed laterally to the four copper bands connecting the neighboring unheated modules. In the process, convection heat transfer would then take over to play the major role of dissipating that heat. The purpose of this configuration was to measure the effect of "exposed" copper foil covered surface area on the heat transfer of the in-line array modules. A new parameter (A^*) was proposed to reflect this effect. The exposed area ratio A^* is defined as:

Table 1. Nusselt Number Variation with Respect to Channel Height for Two Selected Modules and Three Test Boards at Two Different Centerline Velocities.

First Module (Row 1)			Fifth Module (Row 5)		
Channel Height (cm)	Nusselt No.	% increase from H = 7.62 cm	Channel Height (cm)	Nusselt No.	% increase from H = 7.62 cm
1 oz. 2.54 cm Band Width. Channel Air Velocity V = 5 m/s					
7.62	85.7	0	7.62	71.1	0
5.08	92.4	8 %	5.08	83.6	18 %
3.81	98.5	15 %	3.81	91.5	29 %
2 oz. 2.54 cm Band Width. Channel Air Velocity V = 5 m/s					
7.62	98.2	0	7.62	82.6	0
5.08	99.5	1 %	5.08	89.7	9 %
3.81	104.6	7 %	3.81	98.7	19 %
1 oz, 2.54 cm Band Width. Channel Air Velocity V = 11 m/s					
7.62	130.2	0	7.62	105.1	0
5.08	137.7	6 %	5.08	122.4	16 %
3.81	147.8	14 %	3.81	133.7	27 %
2 oz. 2.54 cm Band Width. Channel Air Velocity V = 11 m/s					
7.62	138.3	0	7.62	115.2	0
5.08	151.1	9 %	5.08	130.7	13 %
3.81	154.9	12 %	3.81	141.0	22 %
Adiabatic Board. Channel Air Velocity V = 5 m/s					
7.62	73.2	0	7.62	57.7	0
5.08	76.1	4 %	5.08	67.3	17 %
3.81	82.2	12 %	3.81	74.5	29 %
Adiabatic Board. Channel Air Velocity V = 11 m/s					
7.62	118.4	0	7.62	90.2	0
5.08	119.7	1 %	5.08	107.9	20 %
3.81	130.0	10 %	3.81	115.5	28 %

$$A^* = \frac{\text{Total exposed copper surface area}}{\text{Total exposed area on the board}} \qquad (7)$$

where the total exposed copper surface area is the sum of all the copper bands covered area. The contact surfaces were concealed by the mounted cube modules and were not included. The total exposed area on the board is the surface area of the board minus the sum of all the surface areas occupied by the surface mounted modules. The adiabatic board is a "bare" 1.6 mm (1/16 in.) thick fiber glass board. Corresponding A^* values for the three different copper foil band widths were: 2.54 cm (1 in.) band width, A^* = 0.682; 1.27 cm (0.5in.) band width, A^* = 0.341; and 0.318 cm (0.125 in.) band width, A^* = 0.085.

Figure 9 shows the Nusselt numbers versus row number on four test boards (1 oz boards with three different copper band widths and one adiabatic test board) at four centerline velocities for a fixed channel height of 7.62 cm. Fig. 10 displays the data of three 2 oz conductive and the adiabatic test boards. Nusselt numbers increased with increasing copper band width for a fixed channel height H (7.62 cm) as shown in Figs. 9 and 10. Similar

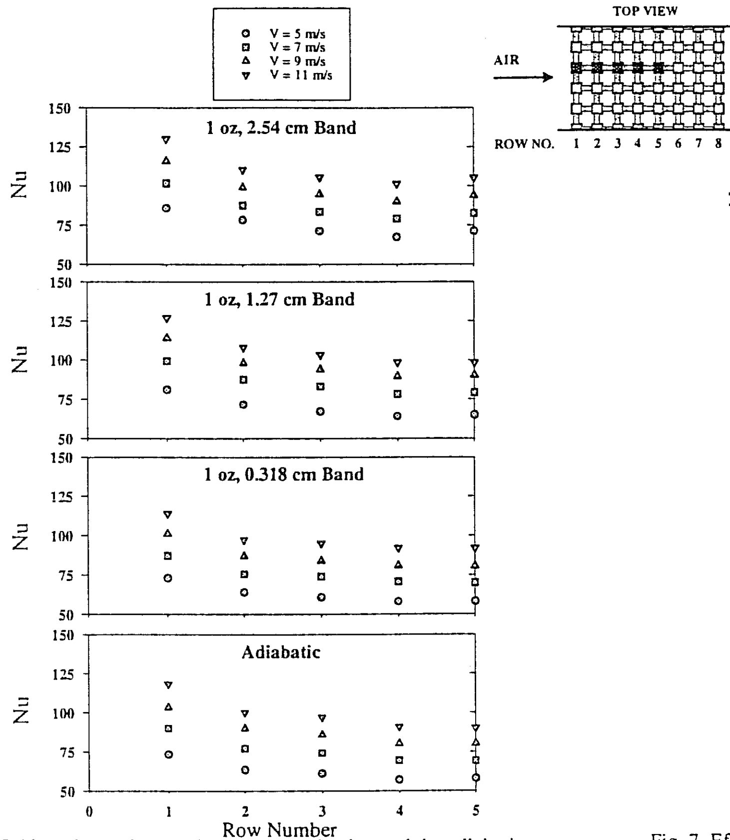

Fig. 5 Nusselt number on three 1 oz conductive and the adiabatic test boards at four different velocities and a channel height of 7.62 cm.

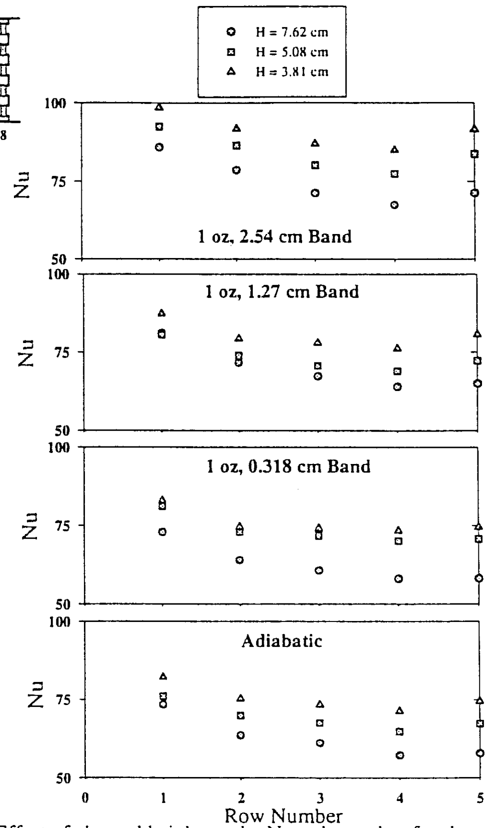

Fig. 7 Effect of channel height on the Nusselt number for three 1 oz conductive and the adiabatic test boards at a channel centerline velocity of V = 5 m/s.

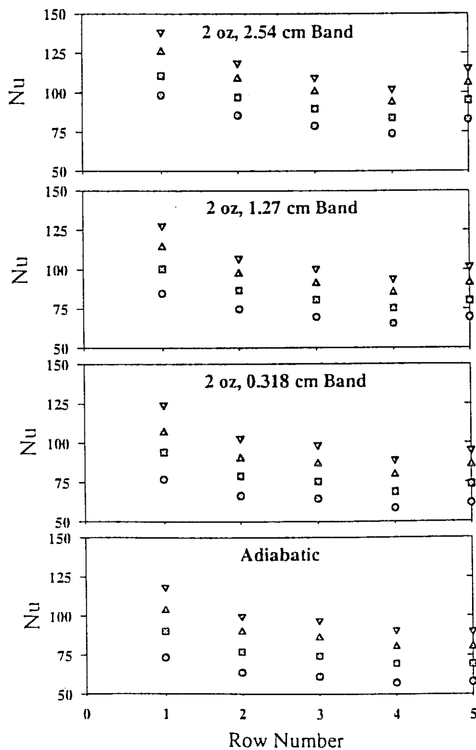

Fig. 6 Nusselt number on three 2 oz conductive and the adiabatic test boards at four different velocities and a channel height of 7.62 cm.

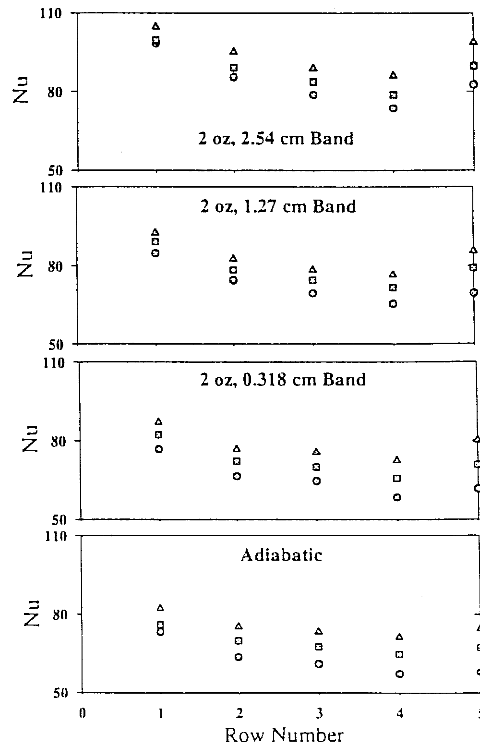

Fig. 8 Effect of channel height on the Nusselt number for three 2 oz conductive and the adiabatic test boards at a channel centerline velocity of 5 m/s.

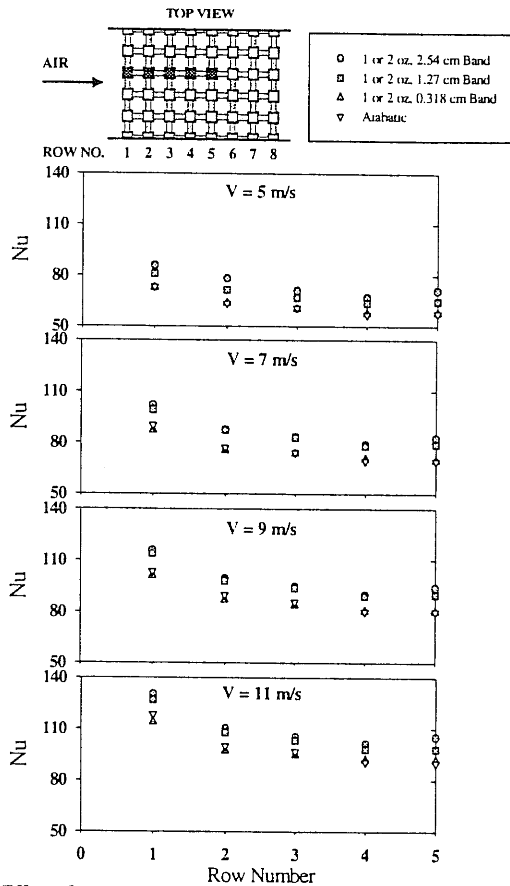

Fig. 9 Effect of copper band width on the Nusselt number for 1 oz conductive test boards at four centerline velocities and a channel height of 7.62 cm.

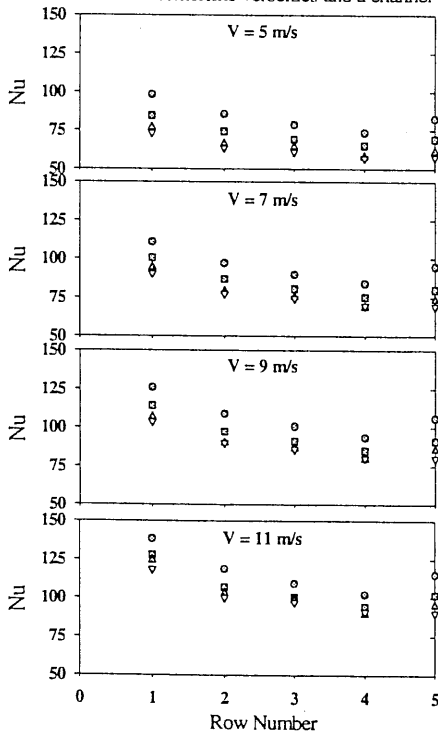

Fig. 10 Effect of copper band width on the Nusselt number for 2 oz conductive test boards at four centerline velocities and a channel height of 7.62 cm.

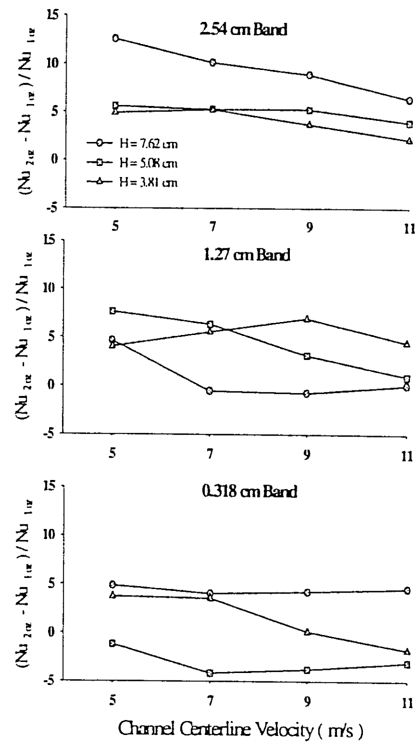

Fig. 11 Average percentage difference of Nusselt numbers of all five test modules between 1 and 2 oz conductive boards at four velocities and three channel heights.

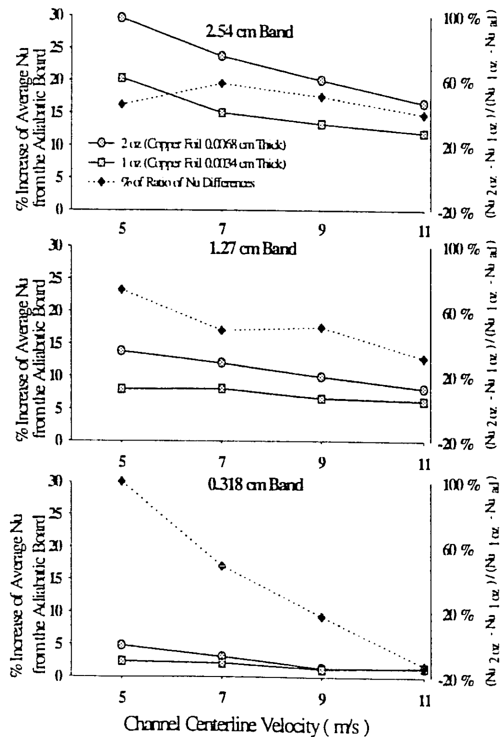

Fig. 12 Percentage increase of the average Nusselt number of three channel heights from the adiabatic board value, and the percentage of the difference of Nusselt number on different test board.

results were found for the other two channel heights. The increases in the convection heat transfer coefficients of the heat dissipating modules were the greatest on the 2.54 cm band ($A^* = 0.682$) conductive test board. The maximum increase was found to be 43% when compared with the Nusselt number on the baseline adiabatic test board at the corresponding conditions (the same channel centerline velocity and channel height). The maximum happened to the fifth module of the heated column on the 2 oz, 2.54 cm band width conductive test board at the channel centerline velocity of 5 m/s for the channel height of 7.62 cm. The increases in the heat transfer coefficients on the average for each conductive board were: 15.1 % on the 1 oz, 2.54 cm band width board; 22.4 % on the 2 oz, 2.54 cm band width board; 7.2 % on the 1 oz, 1.27 cm band width board; 10.9% on the 2 oz, 1.27 cm band width board; 1.8% on the 1 oz, 0.318 cm band width board; and 2.6% on the 2 oz, 0.318 cm band width board.

The comparison between the 0.318 cm band width board and the baseline adiabatic board gave mixed results. Eighteen out of sixty data points (30%) showed that the conductive board with 0.318 cm band width had lower Nusselt numbers than the adiabatic board. There were two possibilities that brought about these eighteen data points. First, the uncertainty of the convection heat transfer coefficients of the study. Secondly, the conditions (channel centerline velocity and ambient air temperature, etc.) of the two test boards when the experiments were conducted were similar but not exactly the same. For 2 oz. 0.318 cm band width, there were twelve points (20%) that showed lower Nusselt numbers than adiabatic board. Not even one of the data points for 2.54 and 1.27 cm band conductive boards had lower Nusselt numbers than the adiabatic board when compared at the same conditions (the same channel height and centerline velocity) with the adiabatic test board. This indicated that the heat transfer behavior of the 0.318 cm band width ($A^* = 0.085$) conductive boards were more toward the adiabatic board ($A^* = 0$) while both the 2.54 cm ($A^* = 0.682$) and 1.27 cm band width ($A^* = 0.391$) conductive boards showed a significant difference in heat transfer behavior when compared with the adiabatic board.

To compliment Figs. 9 and 10, some numerical examples for two selected modules are tabulated in Table 2. The Nusselt number values of the selected modules (first and fifth rows) and the percent variation of the Nusselt numbers with respect to A^* (or copper band width) are listed in Table 2 for three channel heights at a fixed channel centerline velocity of 5 m/s. The same general conclusion drawn from Figs. 9 and 10 can also be drawn from Table 2 that the greater the exposed copper foil surface area ratio (A^*), the higher the Nusselt number of a heat dissipating module.

A common trend shown in Figs. 5 to 10 was that the value of heat transfer coefficient was the highest in the first row and decreased with row number. This trend was reported for modules of cubes by Moffat et al. (1985) and modules of flatpacks by Wirtz and Dykshoorn (1984) for adiabatic cases as well. However, the data displayed in Figs. 6 to 10 show a local maximum at the fifth row in some cases, especially for wider copper foil band widths. Exploratory experiments were conducted to check the inconsistency of the heat transfer coefficients between the fourth and fifth rows. Measurements were taken for the fourth module and then switching the fourth module with the

Table 2. Nusselt Number Variation with Respect to Copper Band Width of Two Selected Modules at Three Channel Heights for a Fixed Centerline Velocity.

First Module (Row 1)				Fifth Module (Row 5)			
Copper Foil Thickness (oz)	Band Width (cm)	Nusselt No.	% increase from the adiabatic board	Copper Foil Thickness (oz)	Band Width (cm)	Nusselt No.	% increase from the adiabatic board
Channel Height H = 7.62 cm, V = 5 m/s							
0	0	73.2	0	0	0	57.7	0
1	0.318	72.8	-0.6 %	1	0.318	58.1	0.7 %
1	1.27	81.0	11 %	1	1.27	66.4	13 %
1	2.54	85.7	17 %	1	2.54	71.1	23 %
2	0.318	76.8	5 %	2	0.318	61.6	7 %
2	1.27	84.6	16 %	2	1.27	69.4	20 %
2	2.54	98.2	34 %	2	2.54	82.6	43 %
Channel Height H = 5.08 cm, V = 5 m/s							
0	0	76.1	0	0	0	67.3	0
1	0.318	81.1	7 %	1	0.318	70.7	5 %
1	1.27	80.5	6 %	1	1.27	72.3	7 %
1	2.54	92.4	22 %	1	2.54	83.6	24 %
2	0.318	82.3	8 %	2	0.318	70.8	5 %
2	1.27	89.1	17 %	2	1.27	79.2	18 %
2	2.54	99.5	31 %	2	2.54	89.7	33 %
Channel Height H = 3.81 cm, V = 5 m/s							
0	0	82.2	0	0	0	74.5	0
1	0.318	82.9	0.9 %	1	0.318	74.5	0
1	1.27	87.3	6 %	1	1.27	80.7	8 %
1	2.54	98.5	20 %	1	2.54	91.5	23 %
2	0.318	87.0	6 %	2	0.318	80.1	8 %
2	1.27	92.4	12 %	2	1.27	85.7	15 %
2	2.54	104.6	27 %	2	2.54	98.7	32 %

fifth module and the results were compared. For selected cases, the difference between Nusselt number of fourth module and Nusselt number of fifth module switched to the fourth row were always less than 3% (the average, 1.7%). This result indicated that the finishing of a module was the most likely explanation for the deviations in the Nusselt number of the fifth module. The bottom surface of the fifth module may have a better contact with the copper foil than the fourth module, thus dissipating more heat through the copper foil.

Effect of Copper Foil Thickness on Nusselt Number

All the conductive test boards used in the study are basically the same. They consist of a thin layer of essentially pure copper laminated to an insulator substrate. Two sets of conductive test boards (1 oz and 2 oz FR-4 Glass Epoxy) with the same copper foil distribution patterns were used. One ounce (1 oz) copper equates to one ounce of copper per one square foot of laminate. In actuality, this means the copper foil is 0.0034 cm thick. Two ounce (2 oz) copper means the copper foil is 0.0068cm thick. The copper foil thickness ratio T* is defined as:

$$T^* = \frac{\text{Copper weight per square foot of the test board}}{\text{Maximum copper weight per square foot (4 oz)}} \quad (8)$$

where maximum copper weight (4 oz) per square foot is the maximum copper weight per square foot (thickest copper foil) generally used for PCBs. Corresponding T^* values for the two different sets of conductive boards were: 1 oz conductive test boards, $T^* = 0.25$; and 2 oz conductive test boards, $T^* = 0.50$.

Increasing the thickness of copper foil on a conductive test board improved the heat transfer of the conductive test board. For

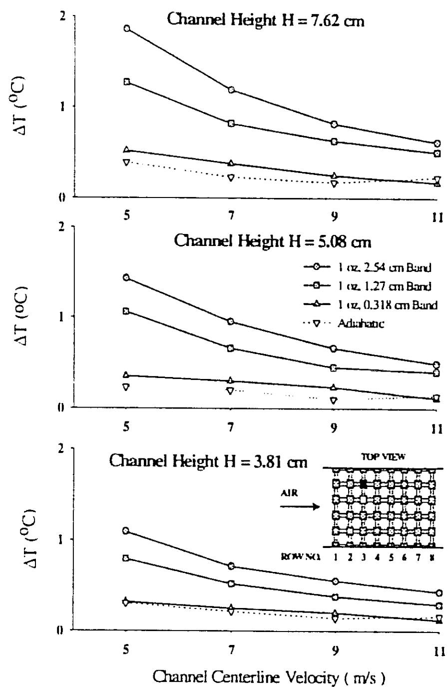

Fig. 13 ΔT of the module to the left (in the flow direction) of the heat dissipating module when it was heated with 20 W for three conductive 1 oz and the adiabatic test boards.

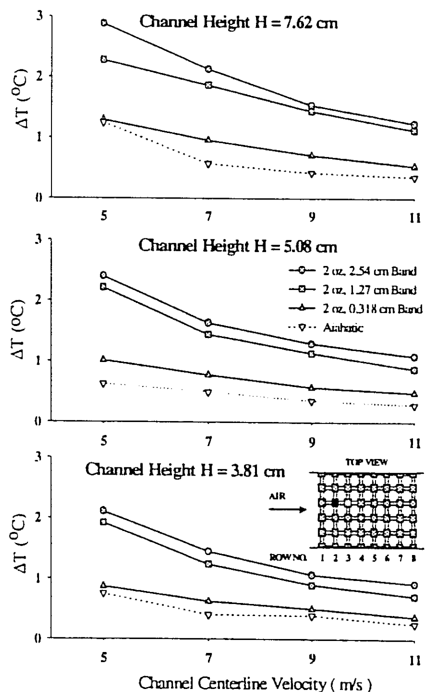

Fig. 14 ΔT of the module upstream of the heat dissipating module when it was heated with 20 W for three conductive 2 oz and the adiabatic test boards.

example, the maximum increase from the adiabatic test board was 24% for 1 oz, 2.54 cm band width and 43% for 2 oz, 2.54 cm band width conductive test board. However, the influence of the thickness of the copper foil was closely associated with the copper foil band width of a conductive test board. The wider the band width, the greater the influence. Secondly, the higher the channel centerline velocity, the less the influence of the thickness of the copper foil. Fig. 11 shows the average percentage difference of Nusselt number of all five test modules between 1 and 2 oz conductive test boards at four velocities and three channel heights. The ranges of the percentage difference were: 2 to 13% for 2.54 cm band width; -1 to 8% for 1.27 cm band width; and -4 to 5% for 0.318 cm band width.

The range was the highest for the 2.54 cm band width and then dropped to the lowest for the 0.318 cm band width. The negative values of the 0.318 cm and, to a lesser degree, 1.27 cm band widths was due to the diminishing influence of the thicker copper foil compounded by the uncertainty of the experiments. The majority of the curves in Fig. 11 also show a downward trend of the influence of the thicker copper foil when the channel centerline velocity increases.

Another perspective to see the influence of copper foil thickness on heat transfer is displayed in Fig. 12. Percentage increase of the average Nusselt number of three channel heights from the adiabatic board value for two sets (different copper foil thicknesses) of conductive test boards are shown in Fig. 12. The downard trends of the increase in Nusselt number with respect to air velocity and copper foil band width can be consistently seen in Fig.12. The ratio of ($Nu_{2\ oz}$ - $Nu_{1\ oz}$) to ($Nu_{1\ oz}$ - Nu_{ad}) in percentage are shown in the figure, too. The averages of the ratios were 50%, 50% and 40% for 2.54, 1.27 and 0.318 cm band widths respectively. This was fairly consistent regardless of copper foil band width. In other words, the enhancement in term of Nusselt number because of thicker copper foil was closely associated with copper foil band width. However, ratio of the "differences" between Nusselt numbers on different test boards offered a different point of view. The enhancement in heat transfer from 1 oz to 2 oz boards relative to the increase from the adiabatic to 1 oz test boards appeared to be fairly uniform among different copper foil band widths.

Effect of Copper Foil Band Width on the Temperature Rises of Neighboring Modules of the Active Module

The temperature rise of a monitored module was defined as the temperature difference between the temperatures of the monitored modules after the third module of the center column was heated with 20W of input power and the temperature of the module when the third module was passive (not heated). The temperatures of all the monitored modules at the lowest ambient temperature when the third module was not heated was designated as the base-line. The temperature rise data for all cases were then generated by subtracting the base-line values of each monitored module from the temperature of each monitored module when the third module was heated. Thus, the temperature rise data would vary with the ambient temperature when each set of data was collected (after the third module was heated and steady state conditions were reached). Because of this, the temperature rise data of each case were further reduced to eliminate the variations of ambient temperature, thus comparisons

among cases can be made. The temperature rise (ΔT) data displayed in Figs. 13 and 14 were the results of subtracting a fixed reference module's temperature rise of each case from the original data. Two neighboring modules of the heat dissipating modules were selected to illustrate the temperature rise results for two copper foil thicknesses.

Figure 13 shows the temperature rises of the module to the left of the heat dissipating module on 1 oz test boards under different conditions and Fig. 14, the upstream module of the heat dissipating module on 2 oz boards. The darkest shaded module in the schematics of the in-line array of modules was the module of interest and the non-shaded module was the module heated with a power level of 20 W. Two clear trends are displayed in Figs. 13 and 14: (1) the wider the copper foil band width, the higher the ΔT, (2) the higher the air velocity, the lower the ΔT. These general observations can be found in three of four neighboring modules of the heat dissipating module. They were the upstream, and modules to the left and right of the active module. Under forced convection heat transfer of the study, the temperature rise results of the downstream module showed a dominant thermal wake effect. The temperature rise data of the downstream module on all test boards clustered together at every channel height. Still, ΔTs of the downstream module decreased when air velocity increased.

Table 3. Steady State Operating Temperature of the Active Module with 20 Watts of Input Power on All Test Boards at a Channel Height and Centerline Velocity.

Channel Height H = 7.62 cm, V = 5 m/s		
Copper Foil Thickness (oz)	Copper Foil Band Width (cm)	Steady State Operating Temperature of the Heat Dissipating Module (20 W) (°C)
0 (Adiabatic)	0	123.3
1	0.318	118.2
1	1.27	109.8
1	2.54	106.2
2	0.318	111.9
2	1.27	108.2
2	2.54	97.7

The temperature rise (ΔT) can be seen as an indicator of the conduction effect of the copper foil. Higher ΔTs of neighboring modules were the result of a better conduction heat spread from the heat dissipating module. Consequently, the active module maintained a lower steady state operating temperature. Some examples of steady state operating temperature are given in Table 3 at a fixed channel height and channel centerline velocity for all seven test boards.

Nusselt Number Correlations

Two correlations presented graphically in Fig. 15 are discussed in this section. These correlations do not represent an attempt to provide empirical correlations for practical applications, but rather to (1) identify the important parameters in the study, (2) capture the characteristics of these parameters and the relationships between them, and (3) demonstrate the collective influences of these parameters on the Nusselt number. The first correlation is:

$$Nu = (0.305 + 0.148A^{*}T^{*} + 0.014\left(\frac{x}{D_h}\right)^{-0.781})\,Re^{0.579} \quad (9)$$

where $0.085 \le A^{*} \le 0.682;\ 0.25 \le T^{*} \le 0.50$
$0.11 \le x/D_h \le 3.64;\ 9100 \le Re \le 26300$

where x is the stream-wise distance from the center of a module to the leading row and D_h is the hydraulic diameter of the rectangular channel at a specific channel height.

The correlation represented the experimental data to within +17% and -16% and had an average absolute deviation of 4.4%. Ninety-two percent of the experimental data (386 data points) were predicted with better than ±10% deviation (see Fig. 15).

To improve the correlation, one more term was introduced into equation (9) to reflect the effect of channel height on the convection heat transfer coefficient. The parameter is a non-dimensional number represented by the channel height (H) divided by the characteristic length of the study, the module height (t). The second correlation is:

$$Nu = (0.496 + 0.238A^{*}T^{*} + 0.022\left(\frac{x}{D_h}\right)^{-0.833})\left(\frac{H}{t}\right)^{-0.111} Re^{0.537} \quad (10)$$

where $0.085 \le A^{*} \le 0.682;\ 0.25 \le T^{*} \le 0.50$
$0.11 \le x/D_h \le 3.64;\ 1.5 \le H/t \le 3.0$
$9100 \le Re \le 26300$

Equation (10) represented the experimental data to within +10% and -16% and had an average absolute deviation of 3.6%. Ninety-six percent of the experimental data (403 data points) were predicted with better than ±10% deviation (see Fig. 15). It can be noticed from Fig. 15 that the addition of H/t improved on the spread of the data points.

Under adiabatic, forced convection conditions, the correlations from previous research were of the general form $Nu = C_1\,Re^{C_2}$. For this study, the ratios of the coefficients of the term $A^{*}T^{*}$ to the leading constant coefficients in both correlations were (0.148/0.305) and (0.238/0.496), respectively. These ratios for both cases were consistently about 49%. Although the coefficient of $A^{*}T^{*}$ was depended on how the A^{*} and T^{*} were defined, the trend shown in the correlations should not be disregarded. This trend indicated that exposed copper foil surface area and thickness of copper foil are two of the most significant parameters in the conjugate heat transfer process.

CONCLUSIONS

Important conclusions from the study are summarized as:

1) The substrate (copper foil) conduction in real PCBs can notably affect the conjugate heat transfer process which clearly should not be neglected. Specific conclusions related to substrate conduction effects are:

- The copper foil bands connecting the heat dissipating module to the surrounding modules played a significant role as the "extended" module surfaces were exposed to the cooling air flow. Thus, the copper foil bands improved the overall convection heat transfer yielding a higher convection heat transfer coefficient of the heat dissipating module. The wider the band width, the greater the improvement on the convection heat transfer coefficient.
- Increase of the copper foil thickness enhances the heat transfer

on real PCBs. However, the increase in heat transfer coefficient was closely associated with the width of the copper foil bands connecting the modules. The wider the band width, the greater the enhancement.

- The copper foil bands of an active module aid in distributing the heat from the heat dissipating module to the lower temperature neighboring passive modules. Consequently, lower steady state operating temperatures were recorded. As a result of wider band widths, the temperature rises of passive neighboring modules also increased considerably. For the adiabatic test board (without any copper foil), this effect was virtually absent, thus the highest steady state operating temperatures were recorded.

2) The modified Reynolds number was one of the most dominant parameters in the study. The flow regimes of all the experiments conducted in this study were turbulent. Accordingly, the Reynolds number governed the conjugate heat transfer process. The following conclusions were revealed by the experimental results considering the modified Reynolds number:

- The higher the modified Reynolds number, the higher the convection heat transfer coefficient of a heat dissipating module. A higher modified Reynolds number was the result of a higher channel centerline air velocity, or a lower channel height, or the combination of both.
- In contrast, the higher the modified Reynolds number, the less significant the conduction effect of the substrate in PCBs. The lower the modified Reynolds number, the more significant the conduction effect of the substrate in PCBs.

3) The most influential parameters in the conjugate heat transfer process were the modified Reynolds number (Re) proposed in this study which took into account the change of cross sectional area associated with different channel heights, the exposed copper surface area ratio (A*), the copper foil thickness ratio (T*), and the non-dimensional channel height (H/t).

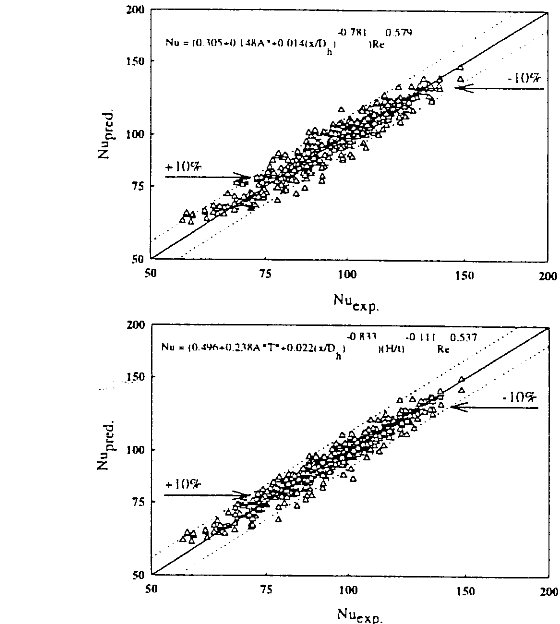

Fig. 15 Nusselt numbers predicted by two different correlations versus Nusselt numbers calculated from experimental data.

REFERENCES

Arabzadeh, M. (1993), "Experimental Study of Geometric Effects and Conduction Loss on Forced Air-Cooling of Regular In-Line Array of Electronic Components," Ph.D. Thesis, Oklahoma State University, Stillwater, Oklahoma.

Arabzadeh, M., Ogden, E.L. and Ghajar, A.J. (1993), "Conduction Heat Transfer Measurements for an Array of Surface Mounted Heated Components," Enhanced Cooling Techniques for Electronics Applications, ASME HTD-Vol. 263, pp. 69-78.

Arvizu, D.E. and Moffat, R.J. (1982), "The Use of Superposition in Calculating Cooling Requirements for Circuit Board Mounted Electronic Components," Proceedings of the32nd Electronic Components Conference, San Diego, CA, pp. 133-144.

Azar, K. and Moffat, R.J. (1991), "Heat Transfer Coefficient and Its Estimation in Electronic Enclosures," Proceedings of the 1991 National Electronics Packaging and Production Conference (East), Boston, MA.

Biber, C.R. and Sammakia, B.G. (1986), "Transport from Discete Heated Components in a Turbulent Channel Flow," ASME Preprint 86-WA/HT-68.

Graham, K. and Witzman, S. (1988), "Analytical Correlation of Thermal Design of Electronic Packages," Cooling Technology for Electronic Equipment, W. Aung, editor, Hemisphere Publishing Corporation, New York, pp. 249-264.

Kline, S.J. and McClintock, F.A. (1953), "Describing Uncertainties in Single-Sample Experiments," Mechanical Engineering, pp. 3-8.

Kraus, A.D. and Bar-Cohen (1983), A., Thermal Analysis and Control of Electronic Equipment, Hemisphere Publishing Corporation, New York.

Lohan, J.M. and Davies, M.R.D. (1996), "Thermal Interaction Between Electronic Components," Heat Transfer in Electronic Equipment, ASME HTD-Vol. 329, pp. 73-82.

Moffat, R.J., Arvizu, D.E. and Ortega, A. (1985), "Cooling Electronic Components: Forced Convection Experiments with an Air-Cooled Array," Heat Transfer in Electronic Equipment, ASME HTD-Vol. 48, pp. 17-27.

Nakayama, W. and Park, S.-H. (1996), "Conjugate Heat Transfer from a Single Surface-Mounted Block to Forced Convective Air Flow in a Channel," Journal of Heat Transfer, Vol. 118, pp. 301-309.

Sparrow, E.M., Niethhammer, J.E. and Chaboki, A. (1982), "Heat Transfer and Pressure Drop Characteristics of Arrays of Rectangular Modules Encountered in Electronic Equipmnt," International Journal of Heat and Mass Transfer, Vol. 25, pp. 961-973.

Wirtz, R.A. and Dykshoorn, P. (1984), "Heat Transfer from Arrays of Flat Packs in Channel Flow," Proceedings of the 4th Annual International Electronics Packaging Society Conference, New York, pp. 318-326.